A REDUCED ORDER MODEL TO ESTIMATING PROPELLER/WING INTERACTION IN SOLAR POWERED AIRCRAFT PRELIMINARY DESIGN

ALESSANDRO BACCHINI

DIMEAS, Politecnico di Torino,
Torino, Italy
alessandro.bacchini@polito.it

ENRICO CESTINO

DIMEAS, Politecnico di Torino,
Torino, Italy
enrico.cestino@polito.it

GIULIO ROMEO

DIMEAS, Politecnico di Torino,
Torino, Italy
giulio.romeo@polito.it

Abstract

The recent improvements in electric motor technology and battery energy density are making electric propulsion a valid alternative for non-conventional aircraft design. The adoption of this new propulsive system is changing the design of new aircrafts and distributed propulsion seems to be a good way to exploit the advantages of electric propulsion. In order to minimize the power required, an efficient aerodynamics coupled with high efficiency propeller capable of working at low Reynolds numbers has to be developed. Reduced order models are useful in the preliminary design phase to define the best thrust distribution because they allow the analysis of different configurations in an acceptable time. The model presented is a modified lifting line that takes into account the flow acceleration due to the propeller disk and the swirl component due to the propeller rotation. The reduced model was validated with available wind tunnel results and applied for the analysis of the lift distribution of the Heliplat solar energy aircraft. Differences between the presented model and a panel code CFD analysis are also illustrated.

Keywords: lifting line, wing-propeller interaction, solar power aircraft, CFD

1. Introduction

Solar powered HALE UAV are becoming increasingly popular because they can provide a revolutionary platform for tasks like Earth monitoring and telecommunications. In order to have maximum flight time and power to the payload, every solar powered HALE UAV needs to have great propulsive efficiency and the lowest possible drag. The procedure to design this kind of aircrafts (Romeo, Frulla, Cestino, & Corsino, 2004) has been based on the energy balance equilibrium between the available solar power and the required power, the former being mainly dependent on the solar cells area installed on the wing and stabilizer, the latter depending on the velocity and total drag of the platform. In order to minimize the power required one should minimize the aerodynamic parameter $C_D/C_L^{3/2}$ mainly reducing induced and parasite drag and on the other side maximizing the propeller efficiency:

$$P_{req}\Big/S_w = \sqrt{\frac{2}{\rho}}\left(\frac{W_{tot}}{S_w}\right)^{3/2}\left(\frac{C_D}{C_L^{\,3/2}}\right)\frac{1}{\eta_{prop}} \tag{1}$$

To maximize the propulsive efficiency we need to accelerate a big quantity of air by a small Δv:

$$\eta_{propulsive} = \frac{propulsive\ power}{rate\ of\ production\ of\ propulsive\ kinetic\ energy} = \frac{Tu_0}{\left(\frac{\dot{m}_e u_e^2}{2} - \frac{\dot{m}_0 u_0^2}{2}\right)} \tag{2}$$

T is the thrust, u_e is the exit flow velocity, u_0 inlet flow velocity, $\dot{m}_e$ and $\dot{m}_0$ the air mass flow rate.

$$T \approx \dot{m}(u_e - u_0) \tag{3}$$

Since:

$$\dot{m}_e \approx \dot{m}_0 \approx \dot{m} \tag{4}$$

We have:

$$\eta_{propulsive} = \frac{\dot{m}(u_e - u_0)u_0}{\frac{\dot{m}}{2}(u_e{}^2 - u_0{}^2)} = \frac{2u_0}{u_0 + u_e} = \frac{2}{1 + \frac{u_e}{u_0}} \tag{5}$$

From this last equation we can see what we said just above: the smaller is u_e the smaller is the $\Delta v = u_e - u_0$ and the higher is the $\eta_{propulsive}$. However in order to produce the same thrust $T = \dot{m}\Delta v$ we need to impress this Δv to a bigger amount of air $\dot{m}$. To do this we could use bigger propellers or having many small propellers. To achieve the second main objective of the solar powered HALE UAV design, that is reducing drag, we need to design it to have the lowest possible viscous drag and the lowest possible induced drag.
Distributed propulsion seems a good way to achieve those two goals because having many propellers we can easily impress a small Δv on a large amount of air and we can place the propellers to have the best circuitation distribution that has the lowest induced drag. Moreover electric technology is well suited for this purpose because electric motors are easily scalable and small motors can have the same efficiency of bigger ones.

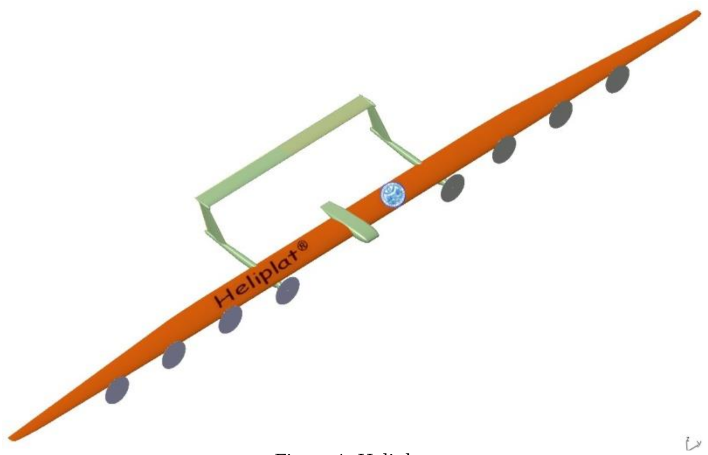

Figure 1: Heliplat

Prandtl's lifting line is the fastest method to estimate the aerodynamic parameters of a 3D wing. It is well suited for the solar powered HALE UAV because of the very high aspect ratios of this kind of aircrafts. To consider propeller's effects, the standard procedure has to be modified inserting the airflow induced by and computing numerically the solution. This has already been done in different ways.
In 1980 J.D. Anderson and S. Corda developed a numerical lifting line method and applied it to pre-stall and post-stall analysis of drooped leading edge wings (Anderson & Stephen Corda, 1980), (Anderson, 2001). This method directly applies the Prandtl equation and after having assumed a circuitation distribution computes numerically the induced angle of attack:

$$\alpha_i(y_n) = \frac{1}{4\pi V_\infty}\int_{-b/2}^{b/2} \frac{\frac{d\Gamma}{dy}}{y_n - y}\,dy \tag{6}$$

And then updates the circuitation guessed applying the Kutta-Joukowski theorem and the definition of lift coefficient:

$$\Gamma(y_n) = \tfrac{1}{2} V_\infty c(y_n) cl(y_n) \tag{7}$$

It is very easy to implement and the propeller induction can be easily modeled as a variation of the V_∞ reaching the wing at the particular position where a propeller accelerates the airflow. However it presents major drawbacks as it is easily subject to numerical errors as the derivative $\frac{d\Gamma}{dy}$ and the denominator $y_n - y$ may tend to diverge when the spacing between stations is small. In 2000 Warren F. Phillips and D. O. Snider proposed another similar method (Phillips & Snyder, 2000). Their idea was to create a semi-panel method with only one panel in the chord wise direction and many panels along the wingspan. The induced velocity is computed as in panels method modifying the formula with some algebra in order to remove a possible division by zero. The tangency condition is not imposed, the algorithm works iteratively until the lift computed with Kutta-Joukowski theorem and the lift computed with the definition of lift coefficient converge to the same value. This formulation allows the lifting line not to be just a simple straight line but to take into account sweep and dihedral angle or strangely shaped wings. However the increased complexity increase the computational load without providing a corresponding increase in accuracy. The method presented in this paper was firstly proposed in (Rakshith, Deshpande, Narasimha, & Praveen, 2015). It is a simple modification of the standard technique applied to solve Prandtl's lifting line. Description of the method and adopted assumption are discussed in detail in the next section.

In the present paper the possibility to preliminary derive aerodynamic properties of the Heliplat solar powered HALE UAV with a reduced order technique based on Prandtl's lifting line theory coupled with a propeller model has been analyzed. The reduced model has been validated by available experimental tests and with the CFD model used for Heliplat's design (Figure 1) developed at Politecnico di Torino by the research group led by Prof. Romeo (Romeo, Frulla, Cestino, & Corsino, 2004).

2. Mathematical model

A modified version of the lifting line theory is used to model the wing-propeller system. The effect of the propeller is taken into account adding to the Prandtl equation the velocity that it induces on the wing. This velocity consists of two components: the axial velocity and the circumferential velocity.

The axial velocity is the velocity induced in the x direction and it is computed with the disk actuator theory:

$$\Delta v = \frac{1}{2}\left[-v_0 + \sqrt{{v_0}^2 + \frac{8T}{\pi\rho D^2}}\right] \tag{8}$$

The circumferential velocity is the velocity induced in the z direction, it is the swirl induced by the propeller (Ferrari, 1957).

$$v_{swirl} = \frac{2v_\infty \Delta v}{\omega r} \tag{9}$$

The aerodynamic parameters of the wing are then computed inserting in the standard Prandtl equation the velocity induced by the propellers.

The wing is subdivided in discrete lifting line segments each one with its own profile, chord and swirl. The lift coefficient of each lifting line segment is computed as:

$$cl = C_{L\alpha}\left(\alpha_{eff} - \alpha_{L=0}\right) \tag{10}$$

Where α_{eff} is the effective angle of attack and takes into account the geometric angle of attack also called flight angle of attack, the twist and the propeller effect:

$$\alpha_{eff} = \alpha_g - \alpha_t - \frac{w_w(y)+w_p(y)}{V(y)} \tag{11}$$

$w_w(y)$ is the downwash induced by the wing still unknown and $w_p(y)$ is the downwash induced by the propeller, earlier called v_{swirl}. The other effect of the propeller, the velocity induced in the x direction is inside $V(y)$. Writing the equality of lift computed as airfoil lift and as 3D vortex lift we find another expression of the lift coefficient:

$$\frac{1}{2}\rho_\infty V(y)^2 c(y) cl(y) = \rho_\infty V(y)\Gamma(\mathrm{y}) \tag{12}$$

$$cl = \frac{2\Gamma(\mathrm{y})}{V(y)c(y)} \tag{13}$$

Then with some more steps we can get to the complete Prandtl equation that takes into account the propellers effect. We rearrange the first cl expression (10) an substitute into it the second one (13):

$$\alpha_{eff} = \frac{cl}{a_0} + \alpha_{L=0} \tag{14}$$

$$\alpha_{eff} = \frac{2\Gamma(\mathrm{y})}{V(y)c(y)C_{L\alpha}} + \alpha_{L=0} \tag{15}$$

Then we insert the induced wing downwash into the effective angle of attack formula (11):

$$w_w(y) = \frac{1}{4\pi}\int_{-b/2}^{b/2}\frac{\frac{d\Gamma}{dy}}{y_0 - y}dy \tag{16}$$

And we finally get the complete Prandtl equation:

$$\frac{2\Gamma(y)}{V(y)c(y)C_{L\alpha}} + \alpha_{L=0} = \alpha_g - \alpha_t - \frac{1}{V(y)}\left[\frac{1}{4\pi}\int_{-b/2}^{b/2}\frac{\frac{d\Gamma}{dy}}{y_0 - y}dy + w_p(y)\right] \tag{17}$$

In order to solve it numerically we proceed with the following coordinate transformation:

$$y = -\frac{b}{2}\cos\theta \tag{18}$$

We assume a circuitation distribution gamma in the form of Fourier series expansion:

$$\Gamma(\theta) = 2bV_\infty\sum_{n=1}^{N}A_n\sin n\theta \tag{19}$$

And we insert it into the Prandtl equation. The derivative of the circuitation distribution is:

$$\frac{d\Gamma}{dy} = \frac{d\Gamma}{d\theta}\frac{d\theta}{dy} = 2bV_\infty\sum_{n=1}^{N}nA_n\cos(n\theta)\frac{d\theta}{dy} \tag{20}$$

Inserting the circuitation distribution and its derivative into the complete Prandtl equation we have:

$$\frac{V_\infty}{V(y)}\frac{4b}{c(y)C_{L\alpha}}\sum_{n=1}^{N}A_n\sin n\theta + \alpha_{L=0} = \alpha_g - \alpha_t - \frac{1}{V(y)}\left[\frac{1}{4\pi}\int_{\pi}^{0}\frac{2bV_\infty\sum_{n=1}^{N}nA_n\cos(n\theta)}{-\frac{b}{2}\cos\theta_0 + \frac{b}{2}\cos\theta}d\theta + w_p(y)\right] \tag{21}$$

Rearranging we have:

$$\frac{V_\infty}{V(y)}\frac{4b}{c(y)C_{L\alpha}}\sum_{n=1}^{N}A_n\sin n\theta = \alpha - \frac{w_p(y)}{V(y)} - \frac{V_\infty}{V(y)}\frac{1}{\pi}\int_{\pi}^{0}\frac{\sum_{n=1}^{N}nA_n\cos(n\theta)}{\cos\theta - \cos\theta_0}d\theta \tag{22}$$

Where α is:

$$\alpha = \alpha_g - \alpha_t - \alpha_{L=0} \tag{23}$$

Introducing the parameter $\mu = \frac{c(y)C_{L\alpha}}{4b}$ and rearranging the previous expressions a final expression can be derived as:

$$\sum_{n=1}^{N}A_n\sin n\theta(\sin\theta + n\mu) = \mu\frac{V_\infty}{V(\theta)}\left(\alpha - \frac{w_p(\theta)}{V(\theta)}\right)\sin\theta \tag{24}$$

The equation above is a system of equations that can be written in matrix form and solved directly with the MATLAB \ solver. Writing it in the standard form we have:

$$\left[\quad M \quad\right]\left\{A\right\} = \left\{b\right\} \tag{25}$$

M is a *m x n* matrix, A is the n x 1 column vector of the Fourier series coefficients and b is a m x 1 column vector.

$$M(m,n) = \sin n\theta_m\left(\sin\theta_m + n\frac{c(\theta_m)C_{L\alpha}}{4b}\right) \tag{26}$$

$$b(m) = \frac{c(\theta_m)C_{L\alpha}}{4b}\frac{V_\infty}{V(\theta_m)}\left(\alpha - \frac{w_p(\theta_m)}{V(\theta_m)}\right)\sin\theta_m \tag{27}$$

Where:

$$m = 1, 2, \dots, M \tag{28}$$

$$n = 1, 2, \dots, N \tag{29}$$

M is the number of stations along the wingspan and N is the number of terms in the Fourier expansion. In order not to have the M matrix singular the number of terms in the Fourier expansion must be smaller than the number of stations along the wingspan, this due to the fact that M is the number of equations of our system and N is the number of unknowns.

The aerodynamic coefficients are then computed with the standard procedure as indicated in (Anderson, 2001):

$$C_L = A_1 \pi AR \tag{30}$$

$$C_{Di} = \pi AR {A_1}^2 \left[1 + \sum_{n=2}^{N} n \left(\frac{A_n}{A_1} \right)^2 \right] \tag{31}$$

The circuitation is computed inserting the A_n into the expression:

$$\Gamma(\theta) = 2bV_\infty \sum_{n=1}^{N} A_n \sin n\theta \tag{32}$$

$$\Gamma(\theta) = \left[\quad G \quad \right] \left\{ A \right\} \tag{33}$$

And the *m x n* matrix G is:

$$M(m, n) = 2bV_\infty \sin n\theta_m \tag{34}$$

The induced angle of attack is computed inserting the A_n into the expression:

$$\alpha_i(\theta) = \sum_{n=1}^{N} nA_n \frac{\sin n\theta}{\sin \theta} \tag{35}$$

$$\alpha_i(\theta) = \left[\quad Z \quad \right] \left\{ A \right\} \tag{36}$$

And the *m x n* matrix Z is:

$$Z(m, n) = n \frac{\sin n\theta}{\sin \theta} \tag{37}$$

3. Validation with experimental data

To evaluate the ability of this method to predict the effects of propeller slipstream, the results were compared with Stuper's wind tunnel data (Stuper, 1938), (Hunsaker & Snyder, 2006). In these experiments the aerodynamics of a rectangular wing (0.8 m span, 0.2 m chord) were studied in the presence of a slipstream. The wing profile was a Gottingen 409 with a lift slope equal to 5.73 and the diameter of the selected propeller was 0.15 m. Three different conditions were compared: wing alone, wing invested by a non-rotational jet and wing-propeller combination. In figure 2 we can see the results of the wing alone configuration, the lift coefficient distribution is plotted for two different angles of attack, 4° and 8°. Predictions obtained by the modified lifting-line method are plotted as a continuous line while the experimental data has been plotted as points. The predictions are quite close to the experimental data, however our model slightly underestimates the Cl especially at high angle of attack. This may be due to our constant $C_{L\alpha}$ parameter computed using Xfoil or to the presence of circular end caps in the experimental model that have a slight winglet type effect. We can see this latter effect in particular in the points close to the wing tips where the experimental lift coefficient is higher than the one predicted by the present model that doesn't consider end caps. The second comparison was performed with a non-rotational slipstream. The freestream speed was 30 m/s, with a jet speed of 35.4 m/s, representing an 18% airspeed acceleration. The thrust was calibrated in the theoretical model in order to obtain the same velocity increase equal to 5.4 m/s. Figure 3 shows the results in terms of lift distribution along the wingspan in the case with irrotational slipstream at two different angles of attack. From this figure we can notice that the modified lifting line model is able to find the effect of the jet. As in figure 2 we can notice the effect of the circular end caps. In figure 4 we can see the lift coefficient plotted along the wingspan for the propeller wing interaction including the rotational effects. propeller's advance ratio is $\lambda = \frac{V_\infty}{\Omega R} = 0.15$, from this parameter the rotational speed of the propeller has been computed. From figure 4 we can notice a very good correlation with the experimental data with a slight overestimation of the propeller effects.

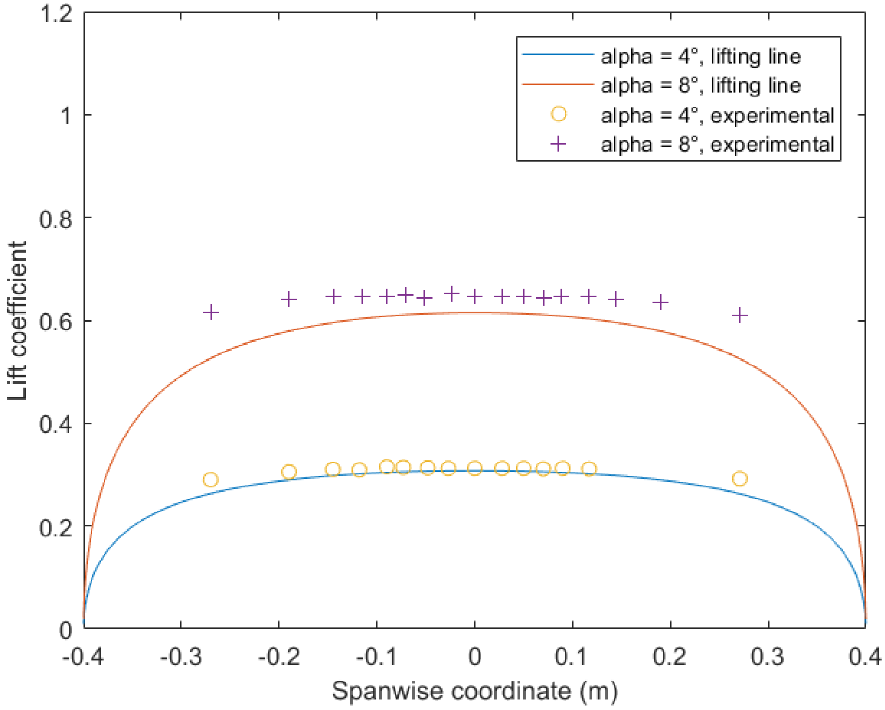

Figure 2: Lift coefficient distribution without propeller slipstream

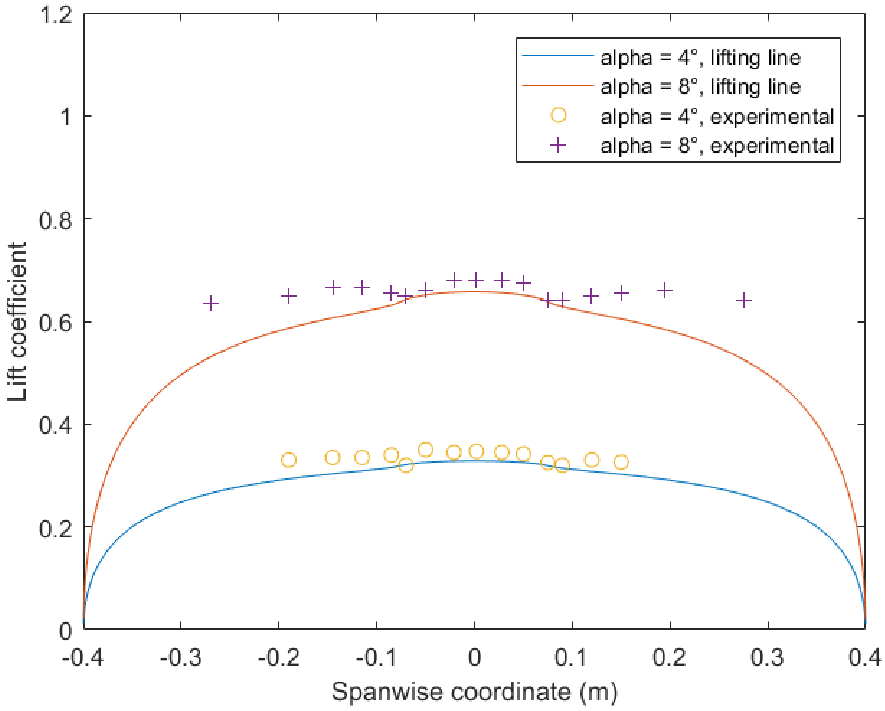

Figure 3: Lift coefficient distribution with active irrotational propeller slipstream

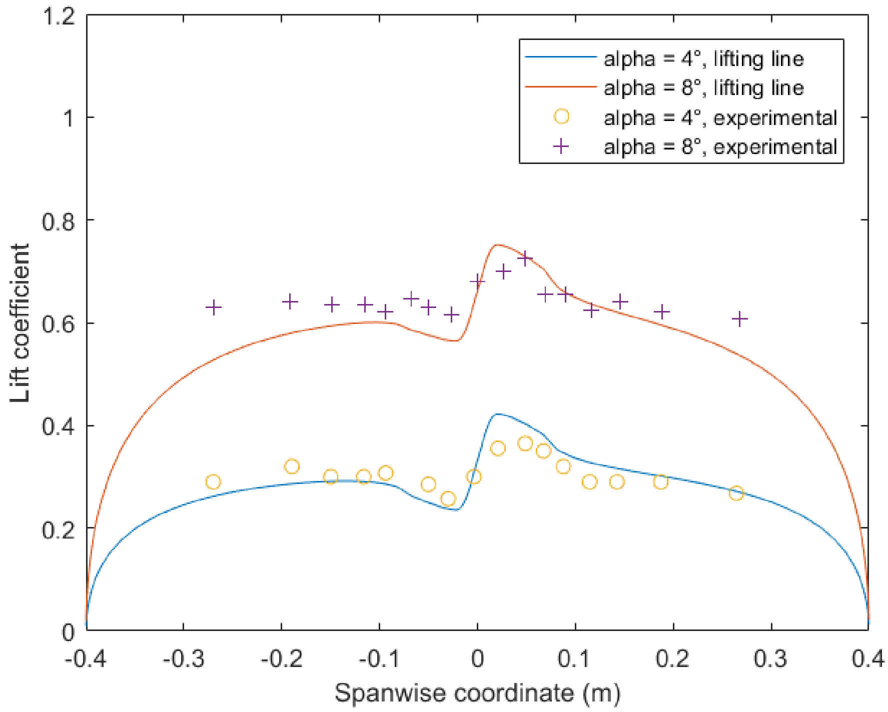

Figure 4: Lift coefficient distribution propeller/wing interaction

4. Application to a Solar HALE configuration

The reduced method was applied to the Heliplat solar powered configuration which main characteristics are summarized in table I. The CFD reference model was developed in VSAERO, a commercial code that calculates the linearized flow external to a body or internal to a duct when the normal velocity on the surfaces bounding the flow is specified: VSAERO solves the Neumann problem of potential flow. Compressibility flow can be analyzed by applying either a Karmann-Tsien correction to the incompressible flow or a Prandtl-Glauert linearization to the compressible flow. The effects of propellers on the aerodynamic behavior of the platform has been included by adding a flow tube wake type plus a swirl membrane to take into account the velocities induced by the propeller rotation (Figure 5).

Table I: input data.

Input data	Numerical value
Root chord	2.96 m
Taper ratio	0.5
Wingspan	73 m
Airspeed	20 m/s
Density	0.1412 kg/m^3
Alpha fly	6°
Alpha 0 lift	-8°
Twist	-2° (linear)
cl-alpha	2π
Number of propellers	8
Diameter	2.3 m
Thrust	23 N
Rotation speed	500 rpm
Spinner radius	23 cm
Number of stations along the wingspan	10000
Number of Fourier modes	300

In figure 6 Heliplat's lift coefficient distribution without propellers computed by VSAERO and by the lifting line method are compared. The main differences are due to the presence of fuselage and the tail boom in the vsaero model. The fuselage is the cause of the Cl drop in the aircraft plane of symmetry, the boom is responsible for the Cl drop at semispan approximately 8 meters from the plane of symmetry. In figure 7 it is reported the same comparison but in the case of activated propellers. Again the lifting line model overestimates the propeller effect compared to the vsaero predictions. Lifting line solution obtained with 1000 span stations and 150 Fourier modes presents some numerical oscillations indicating that better mesh calibration may be found. The differences could be justified by the following reasons:

• As shown in Figure 5b, the VSAERO model is able to evaluate the effect due to the presence of the wing behind the propeller that changes the downstream flow of the propeller (Cf transition from laminar to turbulent flow) that manifests itself in a change in drag that can be considered as an increase in airplane drag or a decrease in the installed thrust of the propeller with the consequence of a lower irrotational induced speed at the propeller disk.

• The reduced model consider a constant behavior of the axial velocity induced by the propeller disk.

• The presence of a body behind the propeller produces a delay in the flow through the propeller disk. An effective propeller advance ratio is frequently introduced, to account for this effect (Schouten, 1999).

• The swirl produces a pressure variation inside the slipstream, leading to a decreased thrust as indicated in (Romeo, Cestino, Pacino, Borello, & Correa, 2012). VSAERO take into account this effect but the reduced model it is not able to capture this variation.

All these differences produce an overestimation of the lift coefficient by the reduced model. It can be concluded that the reduced model is an excellent method that can be adopted in the preliminary design stage even if a more detailed analysis through CFD is still required in order to capture the installation effects.

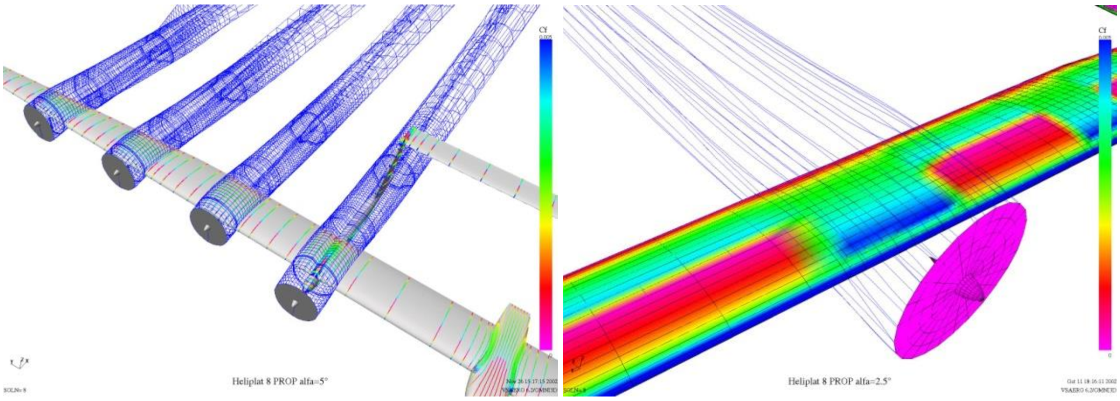

Figure 5: VSAERO Heliplat model with propellers

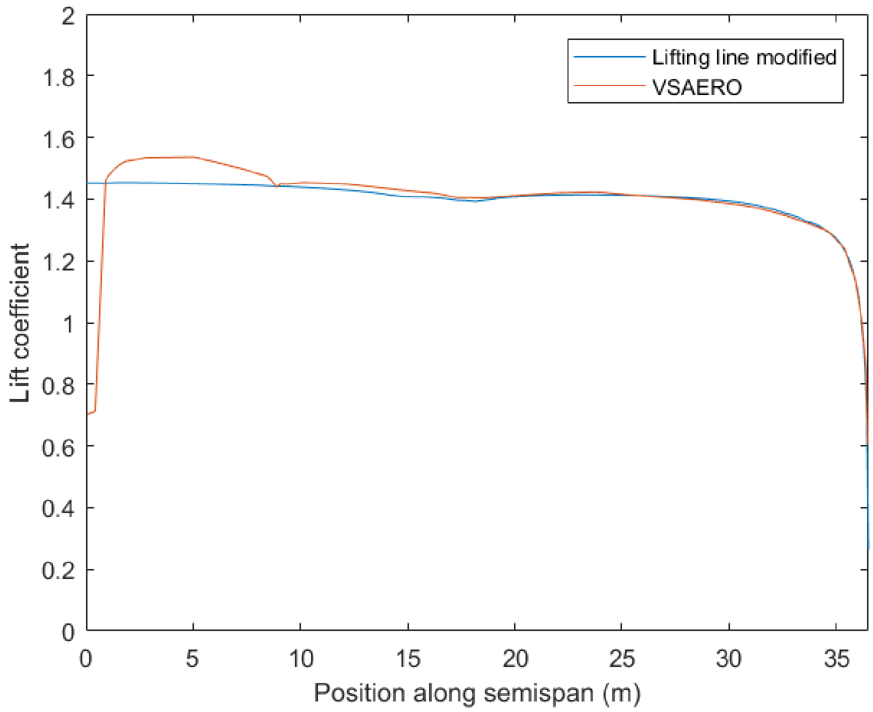

Figure 6: Lift coefficient distribution without propellers

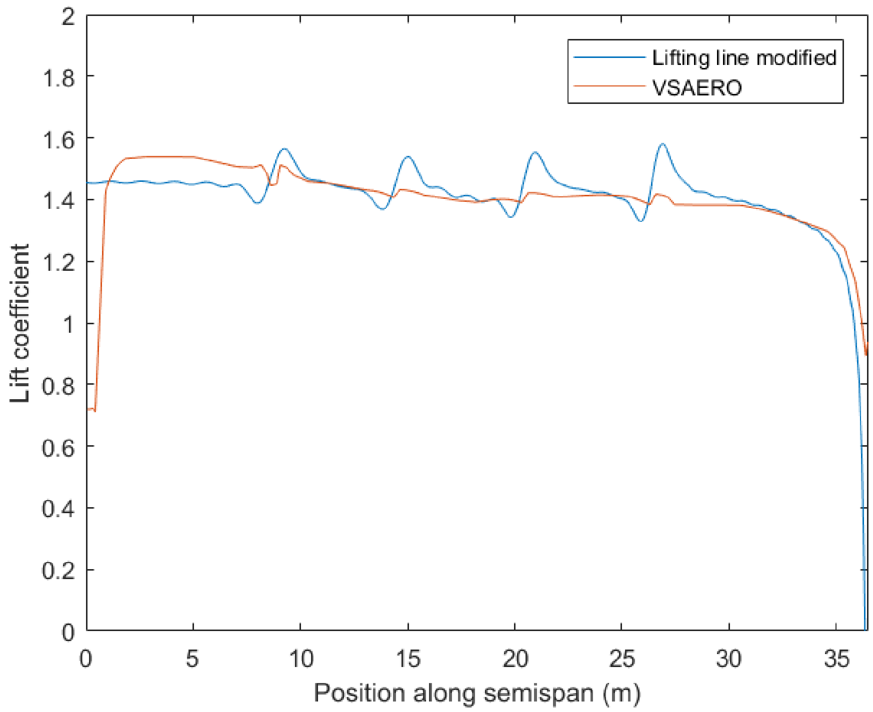

Figure 7: Lift coefficient distribution with propellers

5. Conclusions

A modified Prandtl's lifting line method capable of estimating the aerodynamic coefficients of high aspect ratio wings taking into account the effects of the propellers has been developed and validated with experimental data. A good correlation with wind tunnel data has been obtained by demonstrating the ability to capture the main acceleration and swirl effects due to the presence of propellers on the wing lift distribution. The aerodynamic model developed has the advantage of not being computationally demanding and could be used inside a multidisciplinary optimization process. We found that the low computational cost and no meshing required are very big advantages over more complex methods.

The method presents some limitations due primarily to the inability to take into account the effects of installation and a certain sensitivity of the solution to the number of span subdivisions and the number of Fourier modes adopted. However, the method seems to be promising for its use in the preliminary design phase in order to roughly estimate the effects of wing/propeller interaction facilitating optimal configuration selection. A subsequent detailed CFD analysis is still required to keep secondary effects.

6. References

Anderson, J. D. (2001). *Foundamentals of Aerodynamics.* McGraw-Hill.

Anderson, J. D., & Stephen Corda, M. V. (1980). Numerical lifting line theory applied to drooped leading edge. *Journal of Aircraft vol. 17*, 898-904.

Ferrari, C. (1957). *Interaction Problems, Aerodynamic Components of Aircraft at High Speeds,.* Princeton: Princeton University Press.

Hunsaker, D. F., & Snyder, D. O. (2006). A Lifting-Line Approach to Estimating Propeller/ Wing Interactions. *Utah State University Digital Commons*.

Phillips, W. F., & Snyder, D. O. (2000). Modern Adaptation of Prandtl's Classic Lifting-Line Theory. *Journal of Aircraft vol. 37*, 662-670.

Rakshith, B. R., Deshpande, S. M., Narasimha, R., & Praveen, C. (2015). Optimal Low-Drag Wing Planforms for Tractor-Configuration. *Journal of aircraft*.

Romeo, G., Cestino, E., Pacino, M., Borello, F., & Correa, G. (2012). Design and testing of a propeller for a two-seater aircraft powered by fuel cells. *Proceedings of the Institution of Mechanical Engineers. part G, Journal of Aerospace Engineering, vol. 226 n. 7*, 804-816.

Romeo, G., Frulla, G., Cestino, E., & Corsino, G. (2004). Heliplat: Design, Aerodynamic Structural Analysis of Long-Endurance Solar-Powered Stratospheric Platform. *Journal of Aircraft vol. 41*, 1505-1520.

Schouten, G. (1999). Theodorsen's Propeller Performance with Rollup and Swirl in the Slipstream. *Journal of Aircraft, vol. 36*, 892-895.

Stuper, J. (1938). Effect of Propeller Slipstream on Wing and Tail. *NACA TM 874*.